VI International Conference on Computational Methods in Marine Engineering
MARINE 2015
F. Salvatore, R. Broglia and R. Muscari (Eds)

ON THE SPH MODELING OF FLOW OVER CYLINDER BENEATH TO A FREE-SURFACE

M. Ozbulut*, N. Tofighi*, O. Goren† and M. Yildiz*

*Sabanci University
Faculty of Natural Sciences
Istanbul, Turkey
e-mail: ozbulut@sabanciuniv.edu, web page: http://www.sabanciuniv.edu/

† Istanbul Technical University
Faculty of Naval Architecture and Ocean Engineering
Istanbul, Turkey
e-mail: ogoren@itu.edu.tr - Web page: http://www.itu.edu.tr

Key words: Free Surface Flows, SPH Method, Wave Mechanics, Open Channel Flows

Abstract. This work aims to model flow around rigid cylinder beneath to a free surface by using a particle based Lagrangian method, namely, Smoothed Particle Hydrodynamics (SPH) which has clear advantages on modeling nonlinear violent free surface problems. This problem which is also regarded as 2-d wave making problem in marine hydrodynamics literature is carried out for three different positions of cylinder centre with two different Froude numbers. The fluid motion is governed by continuity and Eulers equations while Weakly Compressible SPH (WCSPH) approximation together with artificial viscosity term is employed for the numerical discretization of the problem domain. Hybrid Velocity-updated XSPH and Articial Particle Displacement (VXSPH+APD) correction algorithm [1] and standard density correction treatment is also added into the numerical scheme. The Reynolds number is chosen as close to 200 for all cases where three dimensionality first starts to be effective in the flow domain [2]. As the flow characteristics are metastable [12], the free-surface deformations, drag and the lift force on the body shows periodic variation during the evolution of the flow. Free-surface deformations at the maximum and minimum lift instants are compared with the results of Reichl et.al. [12] for the first two cases. The last case considers a higher Froude number and deeper cylinder position where lift and drag forces are compared with the findings of [22]. It is observed that the obtained free-surface profiles, mean values of drag and lift forces give consistent results in a good with the referred literature data.

1 INTRODUCTION

Flow past rigid bodies beneath a free-surface has many practical applications in marine engineering like construction of underwater pipelines and offshore structures, modelling the generation of ship bow wave and design processes of submarines. In addition, there is a recent interest on the development of miniature power generators which convert flow energy to electrical energy by using Karman vortex street [6]. Because of the vortex induced vibration forces occurred on the cylinder under uniform current [5], it has a crucial importance to determine the flow characteristics in near and far field of the body by spanning a wide range of Froude numbers and cylinder centre submergence from the free surface. The implementation of the inlet/outlet boundaries and the difficulties on the determination of free surface deformations generated behind the obstacle are mainly two challenging issues to overcome during the numerical modeling of open channel flows over a rigid body. The periodic boundary condition has a critical importance in *(i)*: keeping the mass rate of the flow constant and *(ii)*: providing a uniform flow at the inlet/outlet boundaries of the channel. On the other hand, because of the nonlinear boundary conditions at the unknown free surface, it requires an extensive effort to build a numerical solution model even by neglecting the viscous and rotational effects [4].

There are many experimental, numerical, and theoretical based studies to circumvent these difficulties and enlighten the physics behind the open channel flows around bluff bodies. The earliest attempts to model the free surface (open channel) flows go back to the end of 19^{th} century which was presented by Michell [7] for the calculation of thin ship wave resistance through implementing a perturbation theory. After then there are many attempts to solve ship wave resistance by linear theory together with the wake and trim/sinkage effects [8, 9]. Gadd's formulation is extended by Calisal et.al. [4] and applied to describe the potential flow about a two dimensional, submerged, wing section. Salvesen introduced first and second order theory and compare his results by the experimental findings which has a survey on wide range of submergence and Froude number in his Ph.D. studies [10]. Sheridan et.al. [11] experimentally visualized the vorticity fields which were generated from the cylinder with different Froude numbers and cylinder centre positions at high Reynolds numbers. Reichl et.al. [12] employed a commercial computer program (Fluent) and compare the vorticity patterns qualitatively with the work of aforementioned study of Sheridan et.al. As a mesh-free particle method, Smoothed Particle Hydrodynamics (SPH) [13, 15] is also a very useful tool on the numerical modeling of fluid flows which was successfully validated in bounded channel flows [16, 17] and many open channel and hydraulic problems [19, 20, 22, 23].

The main concern of the present study is to model 2-D wave making problem by using SPH method which is a particle based Lagrangian method and has intrinsic advantages on modeling highly nonlinear violent free surface problems. The flow around a rigid cylinder beneath the free surface problem is solved by utilizing continuity and Euler's equation as governing equations through Weakly Compressible SPH (WCSPH) approach together with an artificial viscosity term. According to WCSPH, the density variations of particles with respect to a reference density value are kept less than %1 so that the fluid can be considered as incompressible. However, the existence of relatively large and random oscillations in the pressure field is the main difficulty associated with the standard WCSPH formulation that needs to be eliminated. In order to circumvent the pressure field related problems, well-known Shepard density filtering algorithm is applied to the numerical scheme. Additionally, an artificial particle displacement (APD) term is added to the position vectors of the fluid particles (except the ones on the free surface) to provide uniform and homogeneous particle distribution during the evolution of the flow which significantly increase the accuracy of the pressure fields [1]. Finally, velocity updated XSPH (VXSPH) treatment is implemented only for the free surface particles which are defined as a very thin layer (1-2 rows).

Reynolds number is taken into account in all infinite fluid flow conditions for the dimensionless analysis which best defines the characteristics of the fluid flows, however, it is not solitarily sufficient to reveal the physical phenomena occur on the open channel flows. The experimental measurements [11] and numerical simulations [12] reveals that the submergence level of the cylinder and Froude number are extensively effective non-dimensional parameters. To compare the behavior of free surface deformations in different flow conditions, Froude number (Fr) and the gap ratio h/d where h is the distance between free surface and cylinder top, d is the diameter of the cylinder should be investigated thoroughly. This work involves a preliminary investigation on the free surface deformations and the forces (lift and drag) on the cylinder body with varying Fr and gap ratios.

The rest of the paper is organized as follows: The governing equations for the fluid flow and SPH numerical scheme used in this work will be presented in the following section together with the applied corrective numerical algorithms. The physical problem parameters, applied boundary conditions and the comparative numerical results will be given in third section. Finally, the concluding remarks and future studies that will be performed on the modeling of open channel flows will be emphasized in the last section.

2 MATHEMATICAL FORMULATIONS

2.1 Governing Equations

In the present study, the flow around a circular cylinder beneath a free surface is solved using continuity and Euler's equation of motion coupled with Lagrangian particle advection. Allowing for fluid element rotation, the governing equations may be specified as

$$\frac{\mathrm{D}\vec{\mathbf{u}}}{\mathrm{D}t} = -\frac{1}{\rho}\nabla P + \vec{\mathbf{g}}, \quad \frac{\mathrm{D}\rho}{\mathrm{D}t} = -\rho\nabla\cdot\vec{\mathbf{u}}, \quad \vec{\mathbf{u}} = \frac{\mathrm{D}\vec{\mathbf{r}}}{\mathrm{D}t}, \tag{1}$$

where $\mathrm{D}/\mathrm{D}t$, ∇, $\vec{\mathbf{u}}, \vec{\mathbf{r}}$, P and ρ are the material time derivative, nabla operator, velocity vector, position, pressure and the density of particles, respectively, while $\vec{\mathbf{g}}$ denotes grav-

itational acceleration vector.
The governing equations are discretized using WCSPH approach. WCSPH method uses an artificial equation of state which couples pressure and density variations through a coefficient commonly known as the speed of sound. There are many types of artificial equation of state used in the WCSPH approximation which enables to calculate the particle pressures to compute the pressure gradient term in the equation of motion. The one proposed by Monaghan [14],

$$p = \frac{\rho_0 c_0^2}{\gamma}\left[\left(\frac{\rho}{\rho_0}\right)^{\gamma} - 1\right], \tag{2}$$

is used in this study where c_0 is the reference speed of sound, γ is the specific heat-ratio of water and is taken equal to 7 while ρ_0 is the reference density which is equal to 1000 (kg/m^3) for fresh water. The value of reference speed of sound is determined by dimensionless Mach (M) number which represents the ratio of fluid and sound velocities. In order to keep density fluctuations close to %1, M should be lower than 0.1 [14].

2.2 SPH Numerical Scheme

As a Lagrangian method, SPH represents the flow field by a finite number of moving particles which carry the characteristic properties of the flow such as mass, position, velocity, momentum, and energy. SPH is based on an interpolation process where the fluid domain is modeled through the interactions of neighboring particles using an analytical function widely referred to as the kernel/weighting function $W(r_{\mathbf{ij}}, h)$. Here, h is the smoothing length and $r_{\mathbf{ij}}$ represents the magnitude of the distance vector given as $\vec{\mathbf{r}}_{\mathbf{ij}} = \vec{\mathbf{r}}_{\mathbf{i}} - \vec{\mathbf{r}}_{\mathbf{j}}$ for particle of interest and its neighboring particle, denoted using boldface subscripts $\mathbf{i}$ and $\mathbf{j}$, respectively while $\vec{\mathbf{r}}_{\mathbf{i}}$ and $\vec{\mathbf{r}}_{\mathbf{j}}$ are the position vectors for the particles. The compactly supported, two dimensional piecewise quintic kernel function is employed in the present study [16]. Any arbitrary continuous function is interpolated as, $A(\vec{\mathbf{r}}_{\mathbf{i}})$, or concisely denoted as $A_{\mathbf{i}}$ in the following manner:

$$A_{\mathbf{i}} \cong \langle A(\vec{\mathbf{r}}_{\mathbf{i}})\rangle \equiv \int_{\Omega} A(\vec{\mathbf{r}}_{\mathbf{j}})\, W(r_{\mathbf{ij}}, h) d^3\vec{\mathbf{r}}_{\mathbf{ij}}, \tag{3}$$

where the angled bracket $\langle\rangle$ denotes the kernel approximation, $d^3\vec{\mathbf{r}}_{\mathbf{ij}}$ is the infinitesimally small volume element inside the domain and Ω represents the total bounded volume of the domain.

The above given SPH approximation is employed to discretize the governing equations of fluid flow where the integral operation over the volume of the bounded domain is replaced by the summation operation over all neighboring particles $\mathbf{j}$ of the particle of interest $\mathbf{i}$. The differential volume element $d^3\vec{\mathbf{r}}_{\mathbf{ij}}$ is also replaced by $m_{\mathbf{j}}/\rho_{\mathbf{j}}$. As a result, the following relations are provided to discretize the Euler's equation of motion and the mass conservation

$$\frac{d\vec{\mathbf{u}}_{\mathbf{i}}}{dt} = -\sum_{j=1}^{N}(\frac{p_{\mathbf{i}}}{\rho_{\mathbf{i}}^2} + \frac{p_{\mathbf{j}}}{\rho_{\mathbf{j}}^2} + \Pi_{\mathbf{ij}})\nabla_{\mathbf{i}} W_{\mathbf{ij}}, \tag{4}$$

$$\frac{d\rho_{\mathbf{i}}}{dt} = \rho_{\mathbf{i}} \sum_{j=1}^{N} \frac{m_{\mathbf{j}}}{\rho_{\mathbf{j}}} \left(\vec{\mathbf{u}}_{\mathbf{i}} - \vec{\mathbf{u}}_{\mathbf{j}}\right) \cdot \nabla_{\mathbf{i}} W_{\mathbf{ij}}. \tag{5}$$

Here, $m_{\mathbf{j}}$ denotes the mass of particle $\mathbf{j}$, $\nabla_{\mathbf{i}}$ is the gradient operator where the particle identifier $\mathbf{i}$ indicates that the spatial derivative is evaluated at particle position $\mathbf{i}$. $\Pi_{\mathbf{ij}}$ is the artificial viscosity term defined as

$$\Pi_{\mathbf{ij}} = \begin{cases} -\alpha\mu_{\mathbf{ij}}\frac{c_{\mathbf{i}}+c_{\mathbf{j}}}{\rho_{\mathbf{i}}+\rho_{\mathbf{j}}}, & \vec{\mathbf{u}}_{\mathbf{ij}} \cdot \vec{\mathbf{r}}_{\mathbf{ij}} < 0 \\ 0, & \vec{\mathbf{u}}_{\mathbf{ij}} \cdot \vec{\mathbf{r}}_{\mathbf{ij}} \geq 0 \end{cases}, \quad \mu_{\mathbf{ij}} = h\frac{(\vec{\mathbf{u}}_{\mathbf{i}} - \vec{\mathbf{u}}_{\mathbf{j}}) \cdot (\vec{\mathbf{r}}_{\mathbf{i}} - \vec{\mathbf{r}}_{\mathbf{j}})}{\left\|\vec{\mathbf{r}}_{\mathbf{i}} - \vec{\mathbf{r}}_{\mathbf{j}}\right\|^2 + \theta h^2}. \tag{6}$$

The inclusion of the artificial viscosity term in the Euler equation of motion is necessary to increase the stability of the numerical procedures through adding some diffusion to numerical solution. The viscosity term added to the momentum equation approximates to the Laplacian of the velocity for incompressible fluids and its limit converges to zero as the spatial resolution increases [21] which is effectively consistent with Euler's equation. In this case, the corresponding numerical kinematic viscosity of the fluid is given theoretically by the relation [14]: $\nu = \alpha c_0 h/8$ which is used in the determination of Reynolds (Re) number in this work.

2.3 Corrective Algorithms

Although it has clear advantages on modeling various fluid flow problems, SPH still needs corrective numerical treatments to reduce particle clustering and noisy pressure field which leads to random and rapid pressure oscillations thereby causing reduced numerical accuracy and stability or even break down of the simulations. Here, density correction and hybrid velocity-updated XSPH and artificial particle displacement (VXSPH+APD) [1] treatments are incorporated into the numerical scheme to circumvent particle clustering induced numerical problems (APD) and provide an artificial stress at the interface that leads to have more precise free surface profiles (VXSPH). The density correction treatment is applied through

$$\widehat{\rho}_{\mathbf{i}} = \rho_{\mathbf{i}} - \sigma\frac{\sum_{j=1}^{N}\left(\rho_{\mathbf{i}} - \rho_{\mathbf{j}}\right) W_{\mathbf{ij}}}{\sum_{j=1}^{N} W_{\mathbf{ij}}}, \tag{7}$$

where $\widehat{\rho}$ is the corrected density, N is the number of neighbor particles for particle $\mathbf{i}$ and σ is a constant which is set to 0.5 in this work thereby leading to the well-known "Shephard" interpolation in SPH literature [24]. The hybrid VXSPH+APD is formulated as

$$\delta \vec{\mathbf{u}}_{\mathbf{i}} = \frac{\sum_{j=1}^{N} (\vec{\mathbf{u}}_{\mathbf{i}} - \vec{\mathbf{u}}_{\mathbf{j}}) W_{\mathbf{ij}}}{\sum_{j=1}^{N} W_{\mathbf{ij}}}, \quad \vec{\mathbf{u}}_{\mathbf{i}}^{xsph} = \vec{\mathbf{u}}_{\mathbf{i}} - \varepsilon \delta \vec{\mathbf{u}}_{\mathbf{i}} \tag{8}$$

$$\delta \vec{\mathbf{r}}_{\mathbf{i}} = \beta \sum_{j=1}^{N} \frac{\vec{\mathbf{r}}_{\mathbf{ij}}}{r_{\mathbf{ij}}^{3}} r_o^2 u_{max} \Delta t, \tag{9}$$

where $\vec{\mathbf{u}}_{\mathbf{i}}^{xsph}$ is called VXSPH velocity and assigned to the new velocity of the free-surface particle, ε is a constant parameter which is taken as 0.001 and u_{max} is the velocity coefficient of the APD assigned as the maximum particle velocity inside the fluid domain. β is a problem dependent parameter which should be small enough not to change the physics of the flow and large enough for providing a homogeneous and uniform particle distribution where it is assigned as 0.005 in the simulations of this work. r_o is an average distance calculated for each particle as $r_o = \sum_{\mathbf{j}} r_{\mathbf{ij}}/N$. In hybrid approach, the VXSPH is applied only to free-surface particles while APD is used to regularize the arrangement of internal particles. These regions are distinguished via kernel truncation. In other words, a particle with fully populated neighboring region has full support and is considered to be an internal particle while particles whose number of neighbors are below certain threshold compared to computational domain average are assigned to the free-surface. On the light of this idea, the particles which has less than (60-70)% of the computational domain average neighbor particle number has been found to describe the free-surface accurately and is used in all calculations involving free-surface values.

3 PROBLEM DEFINITION AND NUMERICAL RESULTS

3.1 Problem Definition

The schematic display of the open channel flows simulated in this work is shown in Fig.1. The dimensionless parameters of the test cases investigated in this study are presented in Table 1. The Froude numbers which has the dominant effect on the generation of free surface waves are given depending on the characteristic length parameters d, h and $\hat{H} = H + h$ as

$$Fr_{\hat{H}} = \frac{U}{\sqrt{g\hat{H}}}, \quad Fr_d = \frac{U}{\sqrt{gd}}, \quad Fr_h = \frac{U}{\sqrt{gh}} \tag{10}$$

where g is the gravitational acceleration taken as 9.81 [m/s^2]. The Reynolds number is determined by $Re = \frac{Ud}{\nu}$. The initial conditions of the fluid flow system is an important issue that should be concerned while modeling open channel flows. There can be two possible methods to have the essential system velocity depending on the test cases. The first one is to start the particles at rest and gradually increase the inlet velocity of the

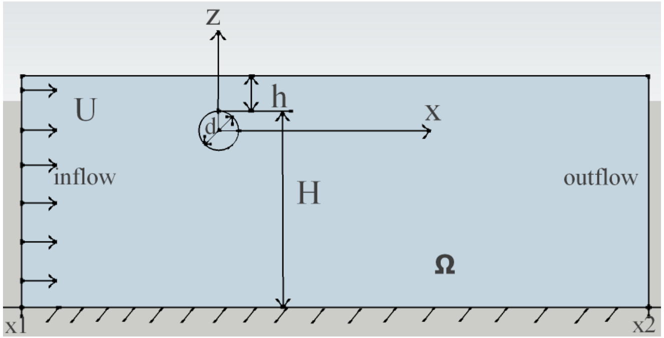

Figure 1: The schematic view of geometric parameters used in the simulations of the open channel flows over a cylinder.

Table 1: Simulation test cases.

H/d	h/d	Re	$Fr_{\hat{H}}$	Fr_d	Fr_h	x_1/d	x_2/d	$\triangle x/d$
9.10	0.40	180	0.13	0.40	0.63	-10	30	0.075
8.95	0.55	180	0.13	0.40	0.54	-10	30	0.075
4.50	2.50	200	0.41	1.00	0.63	-6	26	0.050

system till the flow speed reaches to the required velocity. Although it is an adequate approach to initiate the flow, depending on the Froude number it may take quite a long time to reach the desired speed. The second way of initializing the fluid flow is to start all particles with the required flow speed and wait till the flow attains a steady flow character. The simulations of this work are carried out by the second approach where an initial U velocity is assigned to all fluid particles at $t = 0[s]$.

Another complexity encountered in the numerical modeling of open channel systems is the implementation of inflow/outflow boundary conditions. In order to apply the periodic boundary conditions, buffer regions are generated at the inlet and outlet of the channel (see Fig.2) where the velocity and pressure boundary conditions on these particles are applied. The particles which leaves the problem domain are sent back to the inlet of the channel with the inlet velocity value (U) to keep the total particle amount constant in the domain. Additionally, a radiation condition is implemented to the outlet threshold particles where it is assumed that the outlet region is far away from the cylinder and the vertical velocity components do not vary along the channel length ($\frac{\partial v}{\partial x} = 0$), so that vertical velocity values of the particles in this region are set to zero. The horizontal velocity components are assigned to u=U for the fluid particles in the inlet and outlet buffers.

It is known that SPH has the capability to capture the kinematic and dynamic free surface boundary conditions naturally thereby no additional boundary condition is implemented for the free surface particles [18]. The bottom wall boundary condition is

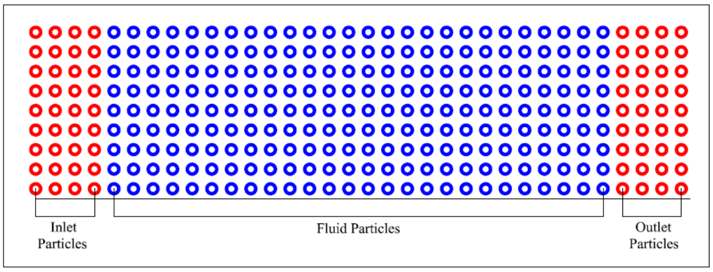

Figure 2: The display of inlet and outlet flow regions.

considered as a free-slip condition [1]. However, to reduce the ground effects and particle discrepancies due to the initial condition of the fluid particles a pseudo-velocity (U) is set to the bottom solid particles where the positions of these particles are not updated with this velocity. On the other hand, Neumann boundary condition is enforced for the solid cylinder particles where an additional pressure is added to the pressure values of these particles which are calculated through the WCSPH numerical scheme. The final pressures of the solid cylinder particles are calculated by

$$\frac{\partial p}{\partial n} = \rho[\frac{Du_s}{Dt} \cdot n], \quad p^s = p + \frac{\partial p}{\partial n} \cdot (r^* - r_s) \tag{11}$$

where Du_s/Dt denotes the total unit force acting on solid particles, p^s is the final pressure value of solid cylinder particles, r^* is the pseudo-displaced position of cylinder particles due to the acting forces and r_s is the fixed positions of cylinder particles.

3.2 Numerical Results

Three flow cases are studied in the present work where each case investigates different submergence level of cylinder centre. In the first two cases, the cylinder centre is quite close to the free surface and the Froude numbers are taken as relatively low (Fr_d=*0.40*). The free surface deformations which can be regarded as one of the kinematical characteristic of the flow is compared with the numerical study of [12] at maximum and minimum lift instants for both submergence level. Figures 3 and 4 display the free surface profiles for the gap ratios 0.40 and 0.55 while Fr_d=*0.40*. It can be said that the SPH results of free surface deformation are compatible with the ones presented by [12]. The third case investigates the lift and drag coefficients in a higher velocity flow regime (Fr_d=*1.00*) where the rigid body is away from the free surface (h/d=*2.5*). The comparative graph of time histories of the lift and drag force coefficients with the study of [22] are presented in Fig.5(a) and Fig.5(b) respectively. According to these plots, the mean values of drag and lift coefficients and the oscillation in lift coefficient is shown in Table 2. It can be said from the figures 5(a) and 5(b) that both of the force components obtained in the present study has a noisy nature which might be due to the low resolution of particles in the domain. However, it can also be implied that the mean values of the drag and lift

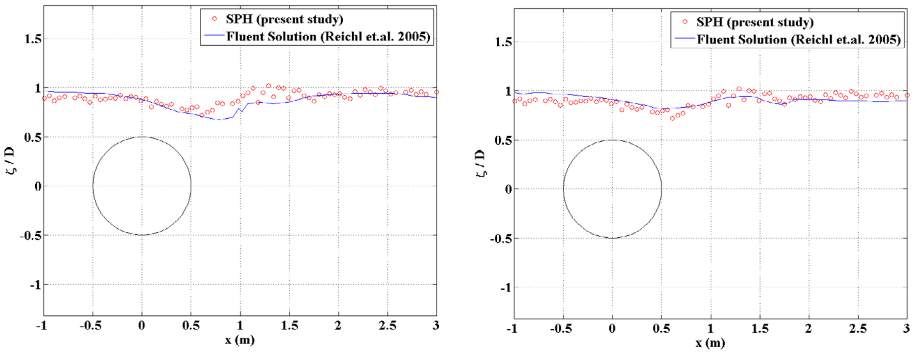

(a) Free surface deformations when the lift is maximum.

(b) Free surface deformations when the lift is minimum.

Figure 3: Comparison of free surface deformations with the results of [12] for *h/d=0.40* and *Fr=0.40* case.

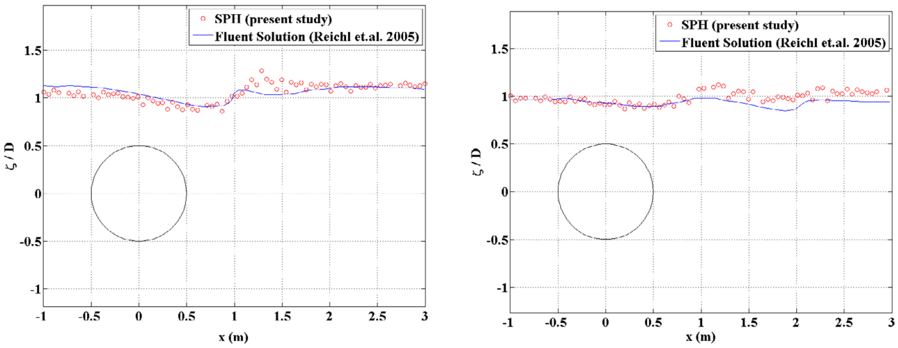

(a) Free surface deformations when the lift is maximum.

(b) Free surface deformations when the lift is minimum.

Figure 4: Comparison of free surface deformations with the results of [12] for *h/d=0.55* and *Fr=0.40* case.

forces are compatible with the referred study and the order of oscillations are compatible with each other.

4 CONCLUDING REMARKS AND FUTURE WORK

The flow around a rigid cylinder beneath the free surface problem is solved by using continuity and Euler's equation as governing equations through Weakly Compressible SPH (WCSPH) approach. In addition to artificial viscosity term proposed by Monaghan [14], the density correction and hybrid velocity-updated XSPH and APD algorithm are included into the numerical scheme. Three submergence positions of the cylinder centre are investigated with two different Froude numbers. In the first two cases, the gap between the cylinder and free surface is quite low (0.40 and 0.50) and the Froude number is equal to 0.40 while the last case covers the higher gap ratio (2.50) and a Froude number (1.00)

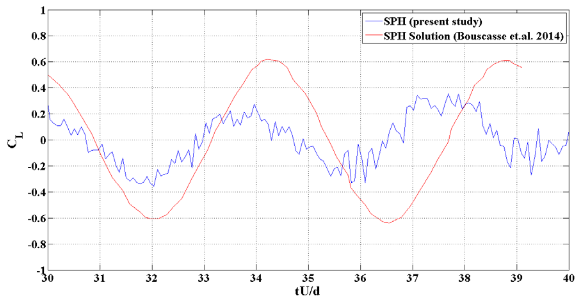

(a) Comparison of time histories of the lift coefficient.

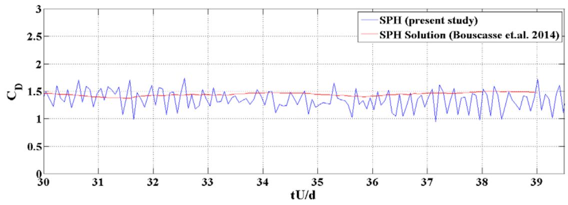

(b) Comparison of time histories of the drag coefficient.

Figure 5: Comparison of lift and drag coefficients with the results of [22].

Table 2: Comparison of drag and lift forces on cylinder.

	h/d	Re	Fr_h	C_D	C_L	C_{Losc}
SPH (present study)	2.5	200	0.63	1.36	0.01	± 0.19
SPH (Bouscasse et.al)	2.5	200	0.63	1.42	0.01	± 0.62

condition. The free surface deformations at maximum and minimum lift instants are compared with the study of [12] where a satisfactory agreement is achieved. The lift and drag coefficients are scrutinized for the last case. It is observed that the lift and drag force components have a little noisy due to the representation of the problem domain with low particle resolution. On the other hand, it can be stated that the magnitudes of the drag and lift coefficients are matching with the literature data.

This work basically considers the general implementation procedures of flow over an obstacle close to a free surface and the preliminary results of the simulations are presented. Although the free surface deformations for relatively low Froude numbers and gap ratios are in accordance with the literature data, the problems faced in the calculations of the drag and lift coefficients should be fixed in order to enlighten the dynamic characteristics of the problem in hand. On the light of the findings of this study, the particle resolution of the fluid domain will be increased and additional test cases will be simulated which involve different submergence and Froude number values in our future studies.

5 ACKNOWLEDGEMENT

The authors gratefully acknowledge financial support provided by the Scientific and Technological Research Council of Turkey (TUBITAK) for project number 112M721.

REFERENCES

[1] Ozbulut, M. Yildiz, M. and Goren, O. A Numerical Investigation into the Correction Algorithms on the SPH Modeling of Violent Free-Surface Flows. *International Journal of Mechanical Sciences* (2014) **79**:56-65.

[2] Barkley, D. and Henderson, R.D. Three-dimensional Floquet stability analysis of the wake of a circular cylinder. *Journal of Fluid Mechanics*, (1996) **322**:215-241.

[3] Reichl, P. Hourigan, K. and Thompson, M.C. Flow Past a Cylinder Close to a Free Surface. *Journal of Fluid Mechanics*, (2005) **533**:269-296.

[4] Calisal, S.M. Goren, O. and Okan, B. On an Iterative solution for Nonlinear Wave Calculations. *Journal of Ship Research*, (1991) **35**:9-14.

[5] Williamson, C. and Govardhan, R. Vortex-induced Vibrations. *Annual Reviews of Fluid Mechanics*, (2004) **36**(1):413-455.

[6] Nguyen, H.D.T., Pham, H.T. and Wang, D.A. A miniature pneumatic energy generator using Karman vortex street. *Journal of Wind Engineering and Industrial Aerodynamics*, (2013) **116**:40-48.

[7] Michell, J.H. The Wave Resistance of a Ship. *Philosophical Magazine*, (1898) **45**:106-123.

[8] Dawson, C.W. A Practical computer Method for Solving Ship Wave Problems. *Second International Conference on Numerical Ship Hydrodynamics*, (1977) University of California, 30-38.

[9] Gadd, G.E. A Convenient Method for Estimating Wave Resistance and Its Variation with Small Changes of Hull Shape for a Wide Range of Ship Types. *International Shipbuilding Progress*, (1981) **28**:262.

[10] Salvesen, N. On Second Order Wave Theory for Submerged Two dimensional Bodies. *University of Michigan*, (1966) Ph.D Thesis, Department of Naval Architecture and Marine Engineering.

[11] Sheridan, J. Lin. J.C. and Rockwell, D. Flow Past a Cylinder Close to a Free Surface. *Journal of Fluid Mechanics*, (1997) **330**:1-30.

[12] Reichl, P. Hourigan, K. and Thompson, M.C. Flow Past a Cylinder Close to a Free Surface. *Journal of Fluid Mechanics*, (1997) **533**(6):269-296.

[13] Gingold, R.A. and Monaghan, J.J. Smooth particle hydrodynamics: theory and application to non-spherical stars. *Astronomical Journal*, (1977) **181**:375-389.

[14] Monaghan, J.J. and Kos, A. Solitary Waves on a Cretan Beach. *Journal of Waterway, Port, Coastal and Ocean Engineering*, (1999) **125**(3):145-154.

[15] Lucy, L.B. A numerical approach to the testing of the ssion hypothesis. *Monthly Notices of the Royal Astronomical Society*, (1977) **181**:375-389.

[16] Shadloo, M.S. Zainali, A. Sadek, S.H. and Yildiz, M. Improved Incompressible Smoothed Particle Hydrodynamics method for simulating ow around bluff bodies. *Computational Methods in Applied Mechanical Engineering*, (1977) **181**:375-389.

[17] Marrone, S. Colagrossi, A. Antuono, M. Colicchio, G. Graziani, G. An accurate SPH modeling of viscous ows around bodies at low and moderate Reynolds numbers. *Journal of Computational Physics*, (2013) **245**:456-475.

[18] Colagrossi, A. Antuono, Le Touze, D. Theoretical considerations on the free surface role in the SPH model and moderate Reynolds numbers. *Physical Review E*, (2009) **79**(056701):1-13.

[19] Federico, I. Marrone, S. Colagrossi, Aristodemo, F. A. Antuono, M. Simulating 2D open-channel flows through an SPH model. *European Journal of Mechanics B/Fluids*, (2012) **34**:35-46.

[20] Songdong, S. Incompressible SPH simulation of wave breaking and overtopping with turbulence modelling. *International Journal for Numerical Methods in Fluids*, (2006) **50**:597-621.

[21] Antuono, M. Colagrossi, A. Marrone, S. and Lugni, C. Propagation of gravity waves through an SPH scheme with numerical diffusive terms. *Computer Physics Communications*, (2011) **182**:866-877.

[22] Bouscasse, B. Colagrossi, A. Marrone, S and Iglesias, A.S. Viscous Flow Past a Circular Cylinder Below a Free Surface. *Proceeding of International Conference on Ocean Offshore and Arctic Engineering (OMAE)*, (2014).

[23] Ozbulut, M. Investigation of Violent Free Surface Flows by Using Smoothed Particle Hydrodynamics *Istanbul Technical University*, (2013) Ph.D Thesis (in Turkish), Faculty of Naval Architecture and Ocean Engineering.

[24] Shepard, D. A Two-dimensinal Interpolation Function for irregularly-spaced data. *Proceeding of the 23rd ACM National Conference, New York*, (1968) 517-524.